

Conjugated Polymer Sensors Built on π -Extended Borasiloxane Cages

Wenjun Liu, Maren Pink, and Dongwhan Lee*

Department of Chemistry, Indiana University, 800 East Kirkwood Avenue,
Bloomington, Indiana 47405

Received March 24, 2009; E-mail: dongwhan@indiana.edu

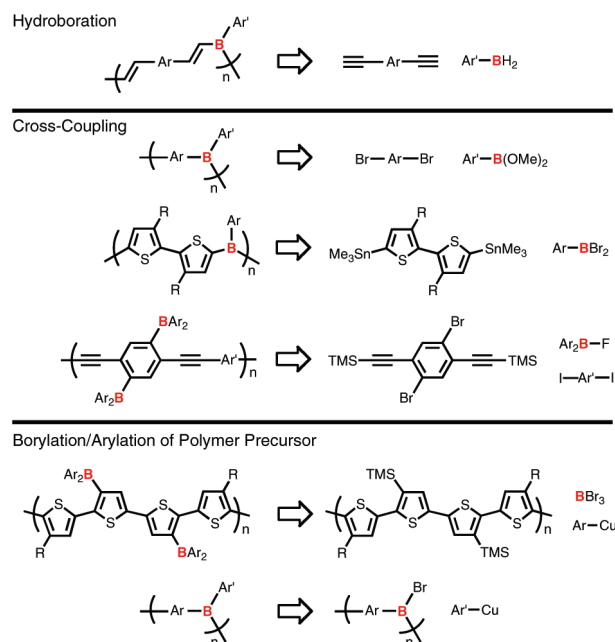
Abstract: An efficient 2 + 2 cyclocondensation with dihydroxysilane converted simple arylboronic acids to bifunctional borasiloxane cage molecules, which were subsequently electropolymerized to furnish air-stable thin films. The extended $[p,\pi]$ -conjugation that defines the rigid backbone of this new conjugated polymer (CP) motif gives rise to longer-wavelength UV-vis transitions upon oxidative doping, the spectral window and intensity of which can be modified by interaction with Lewis basic reagents. Notably, this boron-containing CP undergoes a rapid and reversible color change from green to orange upon exposure to volatile amine samples under ambient conditions. This direct naked-eye detection scheme can best be explained by invoking the reversible B-N dative bond formation that profoundly influences the $p-\pi^*$ orbital overlap.

Introduction

A hybrid structural platform comprising electron-deficient main group elements and electron-rich carbon-based π -conjugation is finding increasing applications in organic functional materials.^{1,2} Simple MO argument dictates that the orientation and occupancy of the p_z -orbital of boron regulate electronic communication between neighboring π -conjugated subunits.^{1,3} As such, modification of this critical $[p,\pi^*]$ -orbital interaction by coordination of a Lewis base profoundly changes the ground-state and excited-state electronic properties of the molecule.⁴⁻⁶ This structure-property relationship has been exploited for an emerging class of boron-containing oligomer and conjugated polymer (CP) sensors,⁷⁻⁹ which are typically constructed by hydroboration,¹⁰⁻¹² cross-coupling with alkenyl/arylborane monomers,¹³⁻¹⁶ or borylation/arylation of polymer precursors (Scheme 1).¹⁶⁻¹⁸

Within this context, we have been searching for alternative design principles to construct boron-containing bifunctional π -systems that are (i) less restricted by functional group

Scheme 1. Representative Boron-Containing CPs and Their Synthetic Precursors



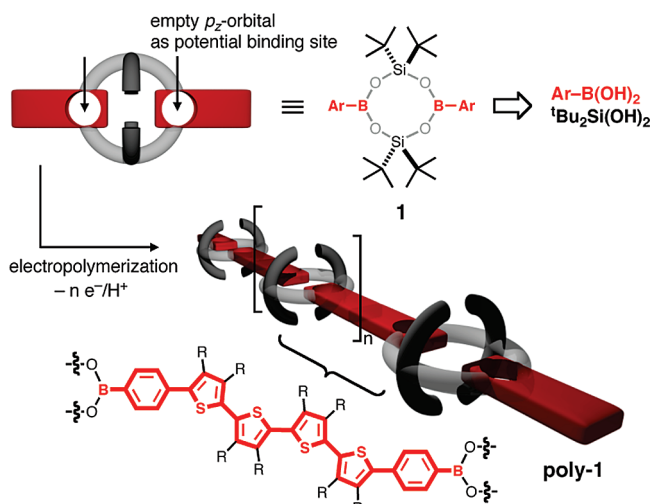
- (1) Elbing, M.; Bazan, G. C. *Angew. Chem., Int. Ed.* **2008**, *47*, 834–838.
- (2) Thematic issue on organic electronics and optoelectronics. *Chem. Rev.* **2007**, *107*, 923–1386.
- (3) Yamaguchi, S.; Tamao, K. *Chem. Lett.* **2005**, *34*, 2–7.
- (4) Yamaguchi, S.; Akiyama, S.; Tamao, K. *J. Am. Chem. Soc.* **2000**, *122*, 6335–6336.
- (5) Yamaguchi, S.; Akiyama, S.; Tamao, K. *J. Am. Chem. Soc.* **2001**, *123*, 11372–11375.
- (6) Yamaguchi, S.; Shirasaka, T.; Akiyama, S.; Tamao, K. *J. Am. Chem. Soc.* **2002**, *124*, 8816–8817.
- (7) Yamaguchi, S.; Wakamiya, A. *Pure Appl. Chem.* **2006**, *78*, 1413–1424.
- (8) Jäckle, F. *Coord. Chem. Rev.* **2006**, *250*, 1107–1121.
- (9) Thomas, S. W., III; Joly, G. D.; Swager, T. M. *Chem. Rev.* **2007**, *107*, 1339–1386.
- (10) Corriu, R. J.-P.; Deforth, T.; Douglas, W. E.; Guerrero, G.; Siebert, W. S. *Chem. Commun.* **1998**, 963–964.
- (11) Matsumi, N.; Naka, K.; Chujo, Y. *J. Am. Chem. Soc.* **1998**, *120*, 5112–5113.
- (12) Matsumi, N.; Miyata, M.; Chujo, Y. *Macromolecules* **1999**, *32*, 4467–4469.

compatibility in synthesis, (ii) modularly constructed by simple condensation of readily available subcomponents, and (iii) readily polymerized to furnish air-stable CPs having tunable optoelectronic properties. In this contribution, we report the synthesis and electropolymerization of linearly conjugated borasiloxane cage molecules¹⁹ to furnish electroactive thin film materials. Interaction between this boron-containing CP and vapor samples of amine elicited a rapid and reversible colorimetric response, thereby allowing direct naked-eye detection.

Results and Discussion

Monomer Design and Synthesis. As a synthetic precursor to boron-containing CP, we targeted a simple borasiloxane cage

Scheme 2. Borasiloxane-Based CP



motif **1** (Scheme 2). From a structural point of view, the eight-membered $\{B_2Si_2O_4\}$ core of **1** serves as a rigid junction that connects two extended π -segments in a linear fashion for subsequent electropolymerization. From a functional point of view, the axial open coordination sites of boron in this construct serve as recognition units capable of binding nucleophilic agents. Previous works elsewhere have produced only a handful of structurally characterized analogues of **1**.^{20–25}

A high-yielding stannylation, cross-coupling, and boronylation synthetic sequence converted bithiophene and bi(EDOT) (EDOT = 3,4-ethylenedioxythiophene) to the corresponding boronic acids **2a** and **2b** (Scheme 3), which were subsequently condensed with $tBu_2Si(OH)_2$ to furnish **1a** and **1b**, respectively.²⁶ The proposed chemical structures of these borasiloxane molecules were supported by 1H - and ^{13}C NMR spectroscopy and high-resolution mass-spectrometry, and unambiguously assigned by X-ray crystallography on **1b**.

As shown in Figure 1, the rigid $\{B_2Si_2O_4\}$ core of **1b** brings the two *p*-phenylene-bi(EDOT) units in close proximity over a $B\cdots B$ distance of 3.997 Å. A through-space electronic coupling between the two π -conjugated fragments across the cage core was also indicated by the UV-vis and fluorescence spectra of

1a, in which both the absorption and emission show systematic red-shifts relative to the isolated chromophore model compound **3a** (Figure S1, Supporting Information).²⁶ This spectroscopic feature is consistent with an exciton coupling between local transition dipoles that are essentially linearly aligned along the $B\cdots B$ vector (Figure 1).²⁷

In addition to serving as convenient 1H NMR handle with chemical shifts far removed from the complicated aromatic region dominated by the rest of the molecule, the bulky *tert*-butyl groups in **1a** and **1b** apparently suppressed the undesired self-condensation of $tBu_2Si(OH)_2$ to siloxanes (pathway B, Scheme 4) or the assembly of unsymmetric borasiloxanes (pathway C, Scheme 4). The boronic acid–boroxine equilibrium (pathway A, Scheme 4),²⁸ established under dehydrating conditions, can be another competing pathway, which is apparently outperformed by the cross-condensation forming stronger Si–O–B bonds with no significant steric strain of the resulting $\{B_2Si_2O_4\}$ ring (Figure 1).

The rigid $\{B_2Si_2O_4\}$ core of **1b** adopts an essentially coplanar arrangement with the adjacent phenylene groups (Figure 1), thereby promoting conjugation between the boron atoms and the arylene backbone. As such, occupation of the vacant *p*-orbital of boron by exogenously added Lewis base was anticipated to influence the optoelectronic properties of the π -extended fragments to which the boron atoms are directly conjugated. The known propensity of boronic esters to bind fluoride ion^{29–32} prompted us to test this idea.

Lewis Acid–Base Interaction of Monomer. Addition of F^- to a THF solution of **1b** elicited a decrease in the intensity of the electronic transitions at $\lambda_{max} = 380$ and 400 nm with concomitant build-up of the blue-shifted feature (Figure 2a). Under similar conditions, the blue fluorescence of **1b** at $\lambda_{max} = 450$ nm ($\lambda_{exc} = 373$ nm) was gradually quenched with an increasing amount of F^- (Figure 2b). Addition of TMSCl (20 equiv with respect to **1b**) to scavenge F^- restored >85% of the original emission intensity, thus confirming that the experimentally observed fluorescence quenching is not a result of irreversible structure disassembly.³³ A broad resonance at -138.9 ppm in the ^{19}F NMR spectrum of **1b** + F^- further confirmed the B–F bond formation in this process.³² The plot of fluorescence intensity monitored at $\lambda = 455$ nm (I_{455}) vs $[F^-]_0$ (Figure 2c) shows an essentially linear decrease in I_{455} with increasing $[F^-]_0$ up to ~ 1 equiv and less pronounced $\Delta I_{455}/[F^-]_0$ afterward, implicating a strong 1:1 binding and a very weak association of the second equiv of F^- . Interdependence of stepwise binding was reported for diboryl receptors,^{34,35}

(13) Matsumi, N.; Naka, K.; Chujo, Y. *J. Am. Chem. Soc.* **1998**, *120*, 10776–10777.

(14) Sundararaman, A.; Victor, M.; Varughese, R.; Jäkle, F. *J. Am. Chem. Soc.* **2005**, *127*, 13748–13749.

(15) Zhao, C.-H.; Wakamiya, A.; Yamaguchi, S. *Macromolecules* **2007**, *40*, 3898–3900.

(16) Li, H.; Jäkle, F. *Angew. Chem., Int. Ed.* **2009**, *48*, 2313–2316.

(17) Li, H.; Sundararaman, A.; Venkatasubbaiah, K.; Jäkle, F. *J. Am. Chem. Soc.* **2007**, *129*, 5792–5793.

(18) For boron-containing CPs based on boronate ester linkages, see: Niu, W.; Smith, M. D.; Lavigne, J. J. *J. Am. Chem. Soc.* **2006**, *128*, 16466–16467.

(19) Höpfl, H. *Struct. Bonding (Berlin)* **2002**, *103*, 1–56.

(20) Mazzah, A.; Haoudi-Mazzah, A.; Noltemeyer, M.; Roesky, H. W. Z. *Anorg. Allg. Chem.* **1991**, *604*, 93–103.

(21) Foucher, D. A.; Lough, A. J.; Manners, I. *Inorg. Chem.* **1992**, *31*, 3034–3043.

(22) Brisdon, B. J.; Mahon, M. F.; Molloy, K. C.; Schofield, P. J. *J. Organomet. Chem.* **1992**, *436*, 11–22.

(23) Beckett, M. A.; Hibbs, D. E.; Hursthouse, M. B.; Malik, K. M. A.; Owen, P.; Varma, K. S. *J. Organomet. Chem.* **2000**, *595*, 241–247.

(24) Avent, A. G.; Lawrence, S. E.; Meehan, M. M.; Russell, T. G.; Spalding, T. R. *Collect. Czech. Chem. Commun.* **2002**, *67*, 1051–1060.

(25) Thieme, K.; Bourke, S. C.; Zheng, J.; MacLachlan, M. J.; Zamanian, F.; Lough, A. J.; Manners, I. *Can. J. Chem.* **2002**, *80*, 1469–1480.

(26) See Supporting Information.

(27) Cantor, C. R.; Schimmel, P. R. *Biophysical Chemistry, Part II*; W. H. Freeman: New York, 1980.

(28) Hall, D. G. In *Boronic Acids: Preparation, Applications in Organic Synthesis and Medicine*; Hall, D. G., Ed.; Wiley-VCH: Weinheim, pp 1–99.

(29) Aldridge, S.; Bresner, C.; Fallis, I. A.; Coles, S. J.; Hursthouse, M. B. *Chem. Commun.* **2002**, 740–741.

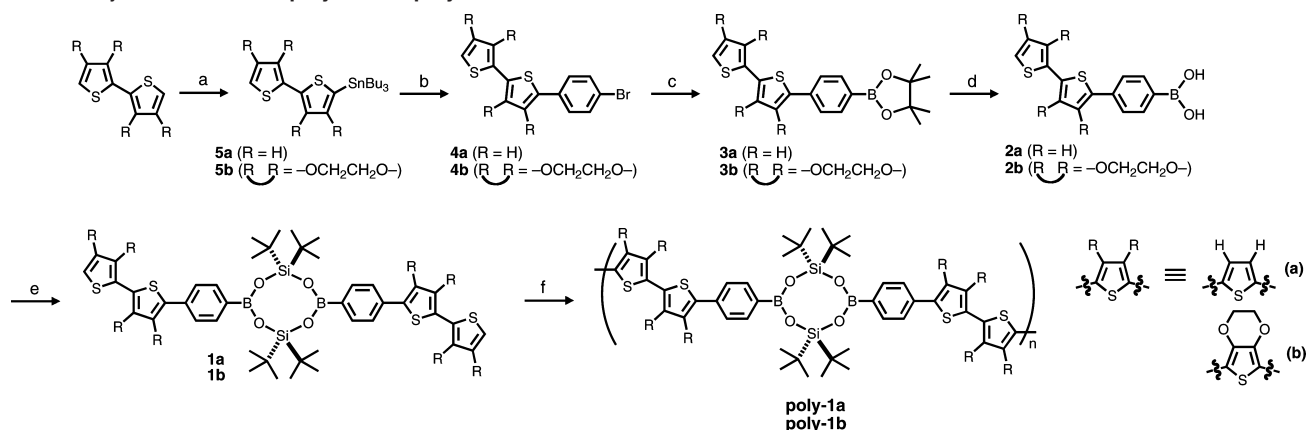
(30) Arimori, S.; Davidson, M. G.; Fyles, T. M.; Hibbert, T. G.; James, T. D.; Kociok-Köhn, G. I. *Chem. Commun.* **2004**, 1640–1641.

(31) Bresner, C.; Day, J. K.; Coombs, N. D.; Fallis, I. A.; Aldridge, S.; Coles, S. J.; Hursthouse, M. B. *Dalton Trans.* **2006**, 3660–3667.

(32) Neumann, T.; Dienes, Y.; Baumgartner, T. *Org. Lett.* **2006**, *8*, 495–497.

(33) Binding-induced spectral change observed in certain boronic ester-based fluoride “sensor” was later confirmed to be the result of irreversible B–O bond cleavage after initial B–F bond formation. See ref 31.

(34) Sundararaman, A.; Venkatasubbaiah, K.; Victor, M.; Zakharov, L. N.; Rheingold, A. L.; Jäkle, F. *J. Am. Chem. Soc.* **2006**, *128*, 16554–16565.

Scheme 3. Synthetic Routes to **poly-1a** and **poly-1b**^a

^a Reagents and conditions: (a) *n*-BuLi, Bu₃SnCl. (b) 1,4-Dibromobenzene, Pd(PPh₃)₄, toluene. (c) Bis(pinacolato)diboron, (dppf)PdCl₂, KOAc, 1,4-dioxane. (d) Aqueous HCl/THF. (e) ^tBu₂Si(OH)₂, toluene, Δ . (f) Anodic polymerization.

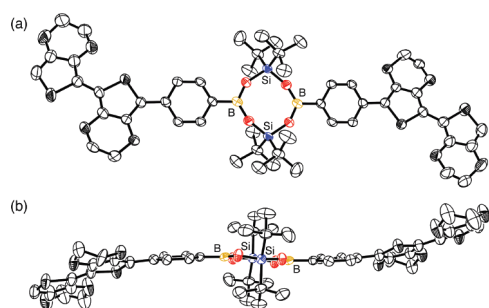
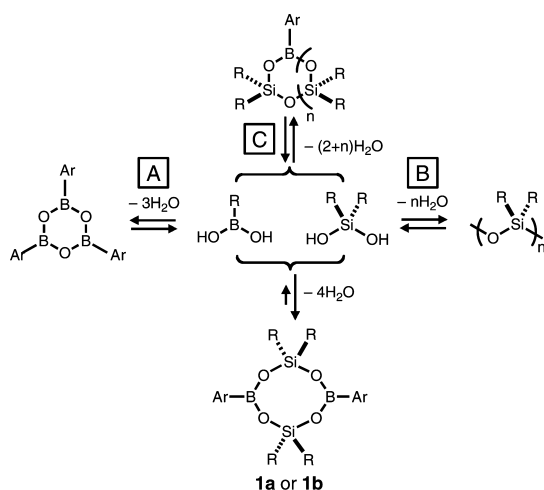


Figure 1. X-ray structure of **1b** with thermal ellipsoids at 50% probability: (a) top view; (b) side view.

Scheme 4. Competing Reaction Pathways in the Assembly of Borasiloxane Cages



which typically display negative cooperativity.^{36–39} With preliminary results obtained for the interaction between the

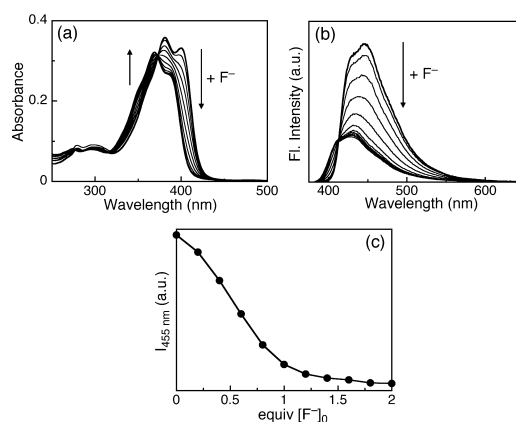


Figure 2. Changes in the (a) UV-vis and (b) fluorescence ($\lambda_{\text{exc}} = 373$ nm) spectra of **1b** (5 μ M) in THF upon addition of F[−] (delivered as *n*-Bu₄NF salt) at 298 K. Each trace corresponds to an increment of 0.2 equiv [F[−]] with respect to **1b**. A plot of fluorescence intensity at 455 nm vs equiv [F[−]]₀ is shown in (c); line was added simply as a guide to the eye.

discrete borasiloxane cage molecule and fluoride ion in solution, we proceeded to explore how such local electronic perturbation would translate to the changes in the optoelectronic properties of their linearly conjugated assemblies.

Electropolymerization. In CH₂Cl₂, **1a** and **1b** show broad irreversible oxidation waves at +0.84 and +0.33 V,⁴⁰ respectively (Figure 3). Repetitive potential sweeps of **1a** (1.0 mM) between 0.0 and 1.3 V (vs Ag/Ag⁺), however, resulted in the deposition of green thin film of **poly-1a** with two broad overlapping features assigned as $E_1^{\text{ox}} = +0.40$ V and $E_2^{\text{ox}} = +0.71$ V. Under similar conditions, anodic polymerization of **1b** furnished **poly-1b** having two well-separated oxidation processes at $E_1^{\text{ox}} = -0.18$ V and $E_2^{\text{ox}} = +0.22$ V, along with a third feature at $E_3^{\text{ox}} = +0.41$ V which became better resolved at slower scan rates (Figure 3).

Cyclic voltammetry (CV) studies on polymer-modified Pt electrodes in monomer-free electrolyte solutions confirmed that these redox activities arise from surface-bound materials with linear dependence of the peak current on the scan rate (Figure S2).²⁶ The electron-donating and sterically hindered ethylenedioxy groups on **poly-1b** not only elicit significant cathodic shifts in the oxidation potential relative to **poly-1a**, but also

(35) Pakkirisamy, T.; Venkatasubbaiah, K.; Kassel, W. S.; Rheingold, A. L.; Jäkle, F. *Organometallics* **2008**, *27*, 3056–3064.

(36) Connors, K. A. *Binding Constants: The Measurement of Molecular Complex Stability*; Wiley: New York, 1987.

(37) Levitzki, A. *Quantitative Aspects of Allosteric Mechanisms*; Springer-Verlag: Berlin, Germany, 1978.

(38) Takeuchi, M.; Ikeda, M.; Sugassaki, A.; Shinkai, S. *Acc. Chem. Res.* **2001**, *34*, 865–873.

(39) Schalley, C., Ed. *Analytical Methods in Supramolecular Chemistry*; Wiley-VCH: Weinheim, 2007.

(40) Unless noted otherwise, all potentials are externally referenced to Cp₂Fe/Cp₂Fe⁺ redox couple.

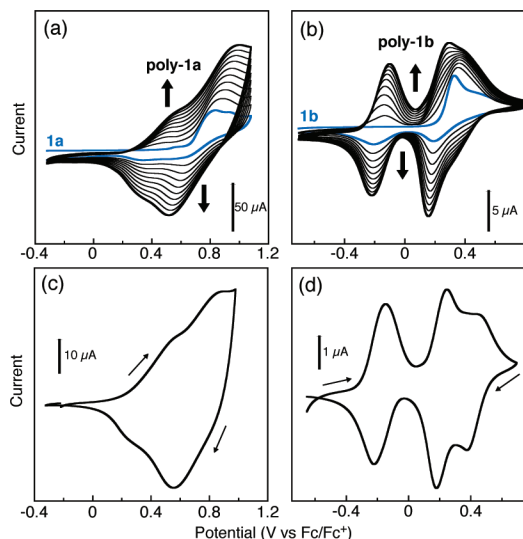


Figure 3. Electropolymerization of (a) **1a** and (b) **1b**, and cyclic voltammograms of the resulting (c) **poly-1a** and (d) **poly-1b** on Pt button electrode in CH_2Cl_2 with $n\text{-Bu}_4\text{NPF}_6$ (0.1 M) as supporting electrolyte. Scan rate = 100 mV/s for (a) and (b); 25 mV/s for (c) and (d). $T = 298$ K.

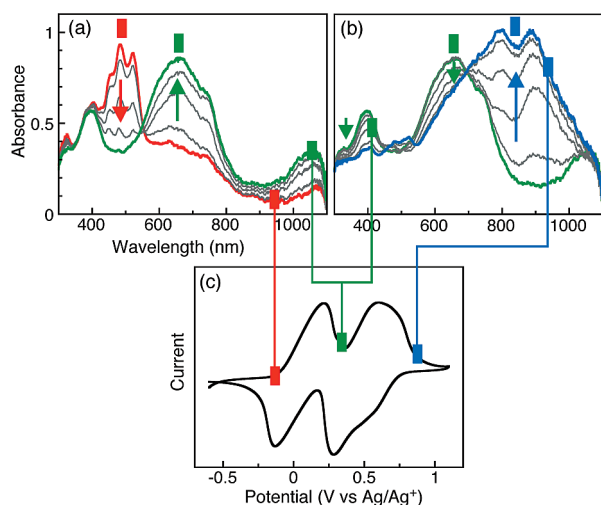


Figure 4. Voltage-dependent changes in the electronic absorption spectra of **poly-1b** on ITO-coated electrode in CH_2Cl_2 (0.1 M $n\text{-Bu}_4\text{NPF}_6$). Each spectral trace corresponds to a 0.1 V increment of applied potential (a) from -0.1 V (red) to $+0.3$ V (green), and (b) from $+0.3$ V (green) to $+0.8$ V (blue). Shown in (c) is the CV of **poly-1b** measured under identical conditions with color-coded rectangles denoting the voltages (referred to Ag/Ag^+) corresponding to the UV-vis spectra in (a) and (b).

assist localization of cationic charge carriers, presumably by suppressing close interstrand contacts required for effective charge delocalization.

UV-Vis Spectroelectrochemistry. The nature of the charge carriers in **poly-1b** was probed further by UV-vis spectroelectrochemistry on polymer-modified ITO electrodes. As shown in Figure 4, **poly-1b** in its fully reduced state displayed electronic transitions with fine vibronic features at $\lambda \approx 480$ nm which is significantly ($\Delta\lambda > 120$ nm) red-shifted compared with that of the monomer **1b** (Figure 2).

Anodic doping within the potential window of $V = -0.1$ to $+0.3$ V (vs Ag/Ag^+), however, resulted in a rapid decay of this $\pi-\pi^*$ transition with concomitant build-up of an intense absorption centered at ~ 650 nm and a color change from orange to green (Figure 4a). A further increase in potential from $+0.3$ to $+0.8$ V (vs Ag/Ag^+) gradually diminished the intensity of this feature with the development of broad near-IR bands which eventually domi-

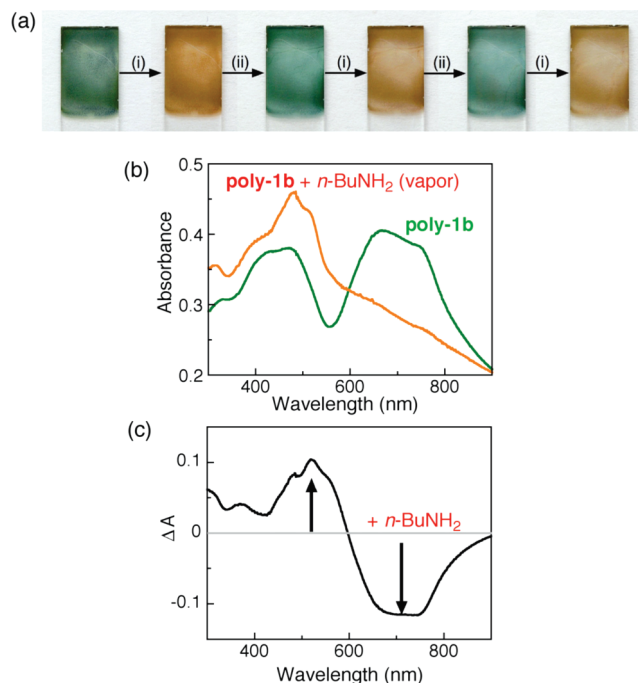


Figure 5. (a) Photographic images of **poly-1b** on ITO-coated glass electrode (width = 0.5 cm) taken after each cycle of (i) exposure to $n\text{-BuNH}_2$ vapor (5 s) followed by (ii) washing with a CH_2Cl_2 solution of $\text{B}(\text{C}_6\text{F}_5)_3$ (5 s). (b) Baseline uncorrected UV-vis spectra of **poly-1b** on ITO-coated glass electrode taken prior to (green) and after (orange) exposure to $n\text{-BuNH}_2$ vapor. (c) Difference spectrum ($\Delta A = A_{\text{poly-1b} + \text{amine}} - A_{\text{poly-1b}}$) generated using the data shown in (b).

nated the UV-vis spectrum of the fully oxidized **poly-1b** (Figure 4b). This voltage-dependent buildup and decay of the systematically red-shifted electronic transitions nicely correlated with the sequential oxidation of **poly-1b** within well-resolved potential windows (Figure 4c), which implicates the evolution of polaronic/bipolaronic states with increasing anodic doping level.^{41–44}

Reversible Colorimetric Response to Amine Vapor. With the electronically conjugated nature of **poly-1b** fully established by CV and UV-vis spectroelectrochemistry, we investigated Lewis acid–base interactions that can potentially modify its extended $[\pi,\pi]$ -conjugation. As shown in Figure 5a, a brief (5 s) exposure of **poly-1b** to a saturated vapor sample of $n\text{-BuNH}_2$ in air resulted in a dramatic color change from green to orange with complete disappearance of the broad longer-wavelength absorption at $\lambda = 550\text{--}800$ nm (Figure 5b). Under similar conditions, either unfunctionalized polythiophene or poly(EDOT) did not show any color change (Figure S3),²⁶ suggesting that the formation of the boron–amine adduct is responsible for the colorimetric response of **poly-1b**. In support of this notion, treating amine-exposed **poly-1b** with a strong Lewis acid $\text{B}(\text{C}_6\text{F}_5)_3$ restored its original green color, and this cycle could be repeated multiple times without noticeable deterioration of

- (41) Roncali, J. *Chem. Rev.* **1992**, *92*, 711–738.
- (42) Skotheim, T. A.; Elsenbaumer, R. L.; Reynolds, J. R., Eds. *Handbook of Conducting Polymers*, 2nd ed.; Marcel Dekker: New York, 1998.
- (43) Fichou, D., Ed. *Handbook of Oligo- and Polythiophenes*, 1st ed.; Wiley-VCH: Weinheim, Germany, 1999.
- (44) Mishra, A.; Ma, C.-Q.; Bäuerle, P. *Chem. Rev.* **2009**, *109*, 1141–1276.
- (45) Key to this visually discernible colorimetric response is the partially oxidized nature of **poly-1b** in air, which gives rise to the intense green color. Neutral **poly-1b**, prepared under N_2 atmosphere and reduced by holding the potential at -0.5 V (vs Ag/Ag^+) for 400 s, retained the orange-yellow color, and exposure to $n\text{-BuNH}_2$ vapor elicited no apparent color change.

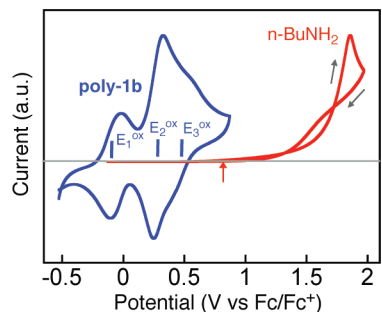


Figure 6. Overlaid cyclic voltammograms of **poly-1b** on Pt button electrode (blue), and *n*-BuNH₂ (red) in MeCN (0.1 M *n*-Bu₄NPF₆) with onset oxidation potential indicated by the red arrow.

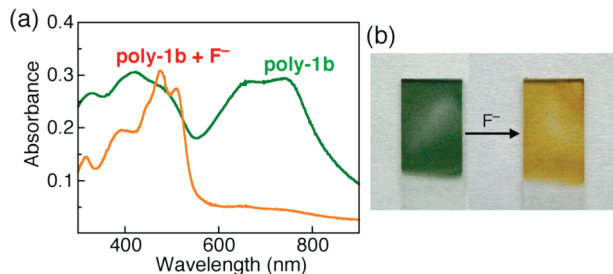


Figure 7. (a) Baseline uncorrected UV–vis spectra of **poly-1b** on ITO-coated glass electrode taken prior to (green) and after (orange) exposure to F[−] (11 mM in THF). (b) Photograph of **poly-1b** on ITO-coated glass electrode (width = 0.5 cm) showing colorimetric response to F[−].

the switching performance (Figure 5a).⁴⁵ Thin films of monomeric **1b** dropcast on ITO showed blue-shift ($\Delta\lambda = \sim 25$ nm) in the absorption peak with no apparent color change upon exposure to *n*-BuNH₂ vapor (Figure S4).²⁶

The experimentally observed color change of **poly-1b** shown in Figure 5 is a consequence of the disappearance of the broad visible absorption at $\lambda \approx 550$ –800 nm. Considering that this longer-wavelength electronic transition is characteristic of the oxidatively doped CP under ambient conditions (Figure 4),^{41,42,45} one could argue that the green-to-orange color change of **poly-1b** might result from chemical reduction of the CP by *n*-BuNH₂. This interpretation, however, contradicts with the findings that (i) the onset potential of the oxidation of *n*-BuNH₂ is > 0.8 V (Figure 6, red arrow), and therefore it is unlikely to function as an outer-sphere chemical reducing agent toward oxidized **poly-1b**; (ii) exposing **poly-1b** to a solution sample of F[−], which cannot function as a chemical reducing agent, elicited similar green-to-orange colorimetric response and UV–vis spectral changes (Figure 7); (iii) reaction of amine-exposed **poly-1b** with the Lewis acid B(C₆F₅)₃, which cannot function as an oxidizing agent, restored the original green color of the polymer (Figure 5a).

In addition, this direct naked-dye detection scheme was applicable for a larger set of sterically unhindered, nitrogen-containing volatile chemicals (Figure 8), the operational generality of which can best be explained by the coordination of Lewis basic ligands to the boron centers in **poly-1b**.⁴⁶ Formation of such a dative B–N bond^{23,47} should remove the boron p_z-orbital from direct conjugation with the π -extended phenyle-

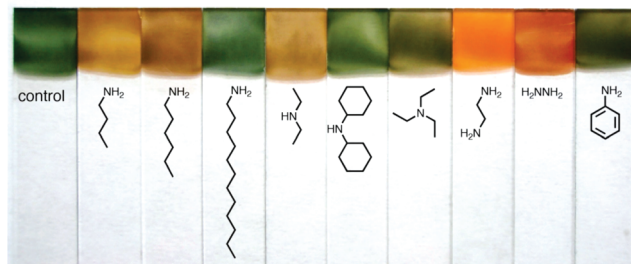


Figure 8. Photographic images of **poly-1b** on ITO-coated glass electrodes taken after exposure to vapor samples of amines under ambient conditions.

nethienylene backbone, and the increased HOMO–LUMO gap could lead to the blue-shift of the polaron/bipolaron transitions of **poly-1b**. This postulation is supported by the difference spectrum shown in Figure 5c, in which a binding-induced decrease in the longer wavelength ($\lambda > 600$ nm) absorption occurs simultaneously with the buildup of new features at the shorter wavelength ($\lambda < 600$ nm).

The response profile shown in Figure 8 apparently reflects the differences in steric and electronic demands of the amine substrates, in addition to their different vapor pressure under ambient conditions. A facile diffusion of the volatile sample into the bulk CP matrix and subsequent formation of stable Lewis acid–base adducts are two important determinants for the sensory performance of **poly-1b**. The contribution of each factor to the collective colorimetric response and the electronic structures that are responsible for such spectral changes are yet to be delineated.

Summary and Outlook

A simple 2 + 2 cyclocondensation with dihydroxysilane converted arylboronic acids to bifunctional cage molecules, which were subsequently electropolymerized to furnish thin film materials responding to volatile amines. Existing CP-based sensors typically rely on changes in electrical resistivity through acid–base chemistry of the polymer backbone,⁴⁸ sorption-induced swelling of CP composites,⁴⁹ or a combination of both⁵⁰ to detect vapor samples of amines. An operationally simple naked-eye detection of volatile amines by **poly-1b** represents an alternative strategy that exploits Lewis acid–base interactions to directly modify the optical properties of CPs. Structural and functional elaboration of this first-generation prototype is currently being pursued in our laboratory in order to improve the sensitivity and selectivity.

Acknowledgment. This work was supported by the U.S. Army Research Office (W911NF-07-1-0533) and the National Science Foundation (CAREER CHE 0547251). D.L. is an Alfred P. Sloan Research Fellow.

Supporting Information Available: Synthesis, characterization, additional electrochemical and spectroscopic data, and crystallographic data. This material is available free of charge via the Internet at <http://pubs.acs.org>.

JA902333P

(46) Oxidation of boron-appended redox-active groups or introduction of cationic charges can enhance the Lewis acidity of organoboron compounds: (a) Venkatasubbaiah, K.; Nowik, I.; Herber, R. H.; Jäkle, F. *Chem. Commun.* **2007**, 2154–2156. (b) Chiu, C.-W.; Kim, Y.; Gabbai, F. P. *J. Am. Chem. Soc.* **2009**, *131*, 60–61.

(47) Ferguson, G.; Lawrence, S. E.; Neville, L. A.; O’Leary, B. J.; Spalding, T. R. *Polyhedron* **2007**, *26*, 2482–2492.

(48) English, J. T.; Deore, B. A.; Freund, M. S. *Sens. Actuators, B* **2006**, *115*, 666–671.

(49) Wang, Y.; Sotzing, G. A.; Weiss, R. A. *Chem. Mater.* **2003**, *15*, 375–377.

(50) Sotzing, G. A.; Phend, J. N.; Grubbs, R. H.; Lewis, N. S. *Chem. Mater.* **2000**, *12*, 593–595.